

# Beam Conditioning for FELs: Consequences and Methods

A. Wolski, G. Penn, A. Sessler, J. Wurtele\*  
*Ernest Orlando Lawrence Berkeley National Laboratory, Berkeley, CA 94720*

October 9<sup>th</sup>, 2003

## Abstract

The consequences of beam conditioning in four example cases (VISA, a Soft X-Ray FEL, LCLS and a "Greenfield" FEL) are examined. It is shown that in emittance limited cases, proper conditioning reduces sensitivity to the transverse emittance, and allows stronger focusing in the undulator. Simulations show higher saturation power, with gain lengths reduced up to a factor of two. The beam dynamics in a general conditioning system are studied, with "matching conditions" derived for achieving conditioning without growth in effective emittance. Various conditioners are considered, and expressions derived for the amount of conditioning provided in each case when the matching conditions are satisfied. We discuss the prospects for conditioners based on laser and plasma systems.

## Disclaimer

This document was prepared as an account of work sponsored by the United States Government. While this document is believed to contain correct information, neither the United States Government nor any agency thereof, nor The Regents of the University of California, nor any of their employees, makes any warranty, express or implied, or assumes any legal responsibility for the accuracy, completeness, or usefulness of any information, apparatus, product, or process disclosed, or represents that its use would not infringe privately owned rights. Reference herein to any specific commercial product, process, or service by its trade name, trademark, manufacturer, or otherwise, does not necessarily constitute or imply its endorsement, recommendation, or favoring by the United States Government or any agency thereof, or The Regents of the University of California. The views and opinions of authors expressed herein do not necessarily state or reflect those of the United States Government or any agency thereof or The Regents of the University of California.

LBNL is an equal opportunities employer.

This work was supported by the Director, Office of Science, of the U.S. Department of Energy under Contract No. DE-AC03-76SF00098.

\*Also at University of California, Berkeley, Department of Physics.

## 1 Introduction

Successful operation of proposed free electron lasers demands electron beams with very small transverse emittance. Particles with large betatron amplitude will tend to slip back with respect to a nominal particle with zero betatron amplitude, and thus can fall out of phase with the radiation produced in an undulator, limiting the gain of an FEL. It has been known for some time that it is possible in principle to ease the requirements on the transverse emittance by introducing a correlation between particle energy and betatron amplitude [1]. Increasing the energy, and hence the longitudinal velocity, of particles with large betatron amplitudes compensates for the phase slip resulting from the betatron amplitude. Thus, an appropriate correlation between betatron amplitude and particle energy in the undulator can ensure that the necessary phase relationship between particles in the beam and the radiation is maintained, allowing FEL operation with larger electron beam emittances than would otherwise be possible.

The analysis in reference [1] was limited to a bunch consisting of particles all having the same longitudinal co-ordinate at the conditioner. Recent work [2] suggested that any attempt to “condition” a non-zero length beam for an FEL by introducing the correct correlation between betatron amplitude and energy inevitably results in an increase in effective transverse emittance. In parameter regimes of interest for proposed facilities, this effective emittance increase was found to be sufficiently large as to prevent any operation of the FEL. Here, we show that these limitations may be avoided, and we present designs of systems where the required conditioning is achieved without increase in effective emittance.

In Section 2 we consider the potential benefits of beam conditioning in the context of proposed and possible facilities, and suggest some interesting parameter regimes. We then proceed in Section 3 to show how conditioning may be achieved without transverse emittance growth, and consider the source of effective emittance growth found by the authors of reference [2]. In Section 4 we give examples of various systems that may be used to achieve conditioning. Finally, in Section 5, we consider laser and laser-plasma conditioners.

## 2 Consequences of Beam Conditioning for FEL Performance

The resonance condition for optimal FEL performance requires a specific average axial velocity: after each undulator period, electrons should fall behind the laser field by exactly one wavelength. The usual resonance condition assumes zero transverse betatron amplitude. For a beam that has non-zero emittance, there is a spread in betatron amplitudes that results in an axial velocity spread which, when too large, limits FEL performance. For FELs that are emittance-limited, more particles can be brought into resonance by introducing a correlation between transverse amplitude and energy.

For a particle having zero transverse amplitude, the average angle inside of an undulator is  $K/\gamma$ , where  $K$  is the normalized strength of the undulator. In the limit of large  $\gamma$ , the angle is roughly the same as  $v_{\perp}/c$ . Thus, averaged over an undulator period, we require:

$$\frac{\bar{v}_z^2}{c^2} = 1 - \frac{1}{\gamma^2} - \frac{\bar{v}_\perp^2}{c^2} = 1 - \frac{1 + K^2}{\gamma^2}.$$

The slippage after one undulator period,  $\lambda_w$ , is given by  $(1 - \bar{v}/c)\lambda_w$ . To be in resonance, this should be equal to the laser wavelength. Using the fact that  $(1 + \bar{v}/c) \approx 2$

$$\lambda = \left(1 - \frac{\bar{v}_z}{c}\right) \lambda_w \approx \frac{1}{2} \left(1 - \frac{\bar{v}_z^2}{c^2}\right) \lambda_w = \frac{1 + K^2}{2\gamma^2} \lambda_w.$$

An electron at non-zero amplitude will have an additional angle  $\theta$  due to its betatron motion. Because the angles due to the betatron motion and the undulator are uncorrelated, they will add in quadrature, leading to an additional term in the slippage of the electron relative to the laser field:

$$1 - \frac{\bar{v}_z^2}{c^2} = \frac{1 + K^2(\bar{r})}{\gamma^2} + \theta^2.$$

The strength of the undulator field will vary off-axis, so there can be an additional effect due to the displacement of the electron. When the focusing is due to the undulator alone, this leads to the condition that:

$$\lambda = \frac{1}{2} \left( \frac{1 + K^2}{\gamma^2} + \frac{2J_x}{\beta_x} + \frac{2J_y}{\beta_y} \right) \lambda_w \quad (1)$$

where  $J_x, J_y$ , are the transverse actions, which in the limit of large  $\gamma$  and small angles are given by:

$$J_x = \frac{1}{2} \left[ \frac{x^2}{\beta_x} + \beta_x \left( \frac{v_x}{c} + \frac{\alpha_x x}{\beta_x} \right)^2 \right]$$

and similarly for  $J_y$ . The average value of  $J_x$  in a beam is equivalent to the geometric emittance  $\epsilon_x$ . Here we assume small  $\alpha_x$  and  $\alpha_y$ .

To maximize the number of particles in resonance, it is necessary to minimize the spread in the RHS of Equation (1). This can be achieved by introducing a correlation of energy with transverse action,

$$\frac{\Delta\gamma}{\gamma} = \kappa_x J_x + \kappa_y J_y,$$

with

$$\kappa_x = \frac{1}{\beta_x} \frac{\gamma^2}{1 + K^2} = \frac{1}{2\beta_x} \frac{\lambda_w}{\lambda},$$

where the original resonance condition has been used and  $\alpha_x$  set to zero. Values of  $\kappa_{x,y}$  required for proper conditioning are typically of the order of  $1 \mu\text{m}^{-1}$ . A value of  $\kappa_x = \kappa_y =$

$1 \mu\text{m}^{-1}$  implies that for a beam with  $1 \mu\text{m}$  normalized emittance in both transverse planes, the typical electron has just over 1 MeV more energy than a zero amplitude particle which is at resonance.

When the beam is more strongly focused, so that  $\beta \ll \gamma\lambda_w/\pi K$ , the variation of magnetic field with position in the bunch is not important. However, when the gain length is shorter than a betatron period, instead of averaging over angle the optimal conditioning is to adjust particles to be resonant at their peak angles, because this occurs when they are close to the axis, which is also where the laser field is strongest. This leads to the same conditioning parameter as above.

Below we consider several examples of FEL parameters to see how conditioned beams perform differently from unconditioned beams. In all cases, the two transverse directions have identical beta functions and we take the conditioning parameter  $\kappa = \kappa_x = \kappa_y$ . The expression for conditioning given above has been verified by simulations to be the optimal value. Note that reducing the beta function of the beam in an FEL requires stronger conditioning for proper matching. Simulations for FEL amplifier performance were performed using the GENESIS code [3].

In the following figures, red is used for the nominal emittance, green for twice the nominal emittance, and black for higher emittances. Points represent unconditioned beams, and lines represent conditioned beams. Because conditioned beams are optimized at smaller beta functions, results using the best value for the beta function for a conditioned beam are represented as lines with ‘+’ symbols. Unconditioned beams should be assumed in the legends unless stated otherwise.

We consider four examples: VISA [4], a soft X-Ray FEL [5], LCLS [6], and a “Greenfield” FEL [7]. Table 1 gives the parameters used in the simulation in each case.

**Table 1**

Parameters used in modeling four FELs.

	VISA	Soft X-Ray	LCLS	Greenfield Low Energy	Greenfield High Energy
Radiation wavelength [nm]	840	1	0.15	0.04	0.04
Electron beam energy [GeV]	0.070	2.5	14.3	12.1	27.8
Fractional energy spread [ $10^{-4}$ ]	8	4	1	1.2	1
Normalized emittance [ $\mu\text{m}$ ]	2.1	2	1.2	0.1	0.1
Peak current [kA]	0.24	0.5	3.4	3.5	3.5
Undulator period [cm]	1.8	2.5	3	3	3
Undulator $K$ parameter	0.89	0.96	2.62	0.71	2.62
Beta function [m]	0.29	4.8	17.5	1.5	1.5
Conditioning parameter [ $\mu\text{m}^{-1}$ ]	0.036	2.6	5.8	22	22

## 2.1 VISA

Results are shown in Figure 1 for various emittances at or above the nominal value, for both conditioned and unconditioned beams. The optimum gain length is roughly 16 cm. It is seen that at nominal values the performance is not limited by emittance, and conditioning has little effect until the emittance is increased by a factor of four.

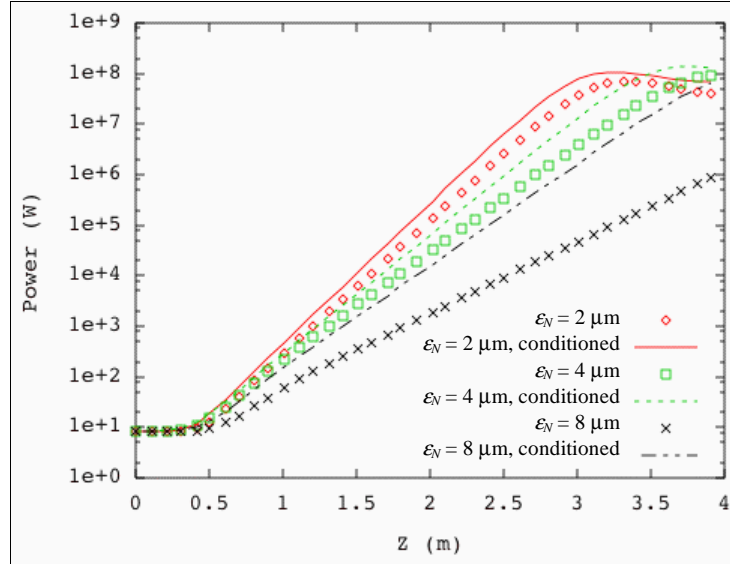


**Figure 1**

Radiation power as a function of undulator length in the VISA FEL. Conditioned and unconditioned beams at different emittances are compared.

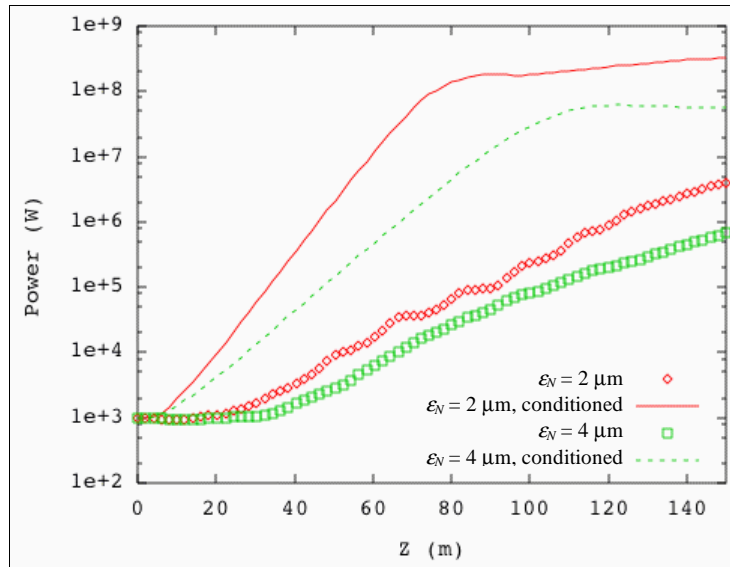


**Figure 2**

Radiation power as a function of undulator length in the Soft X-Ray FEL. Conditioned and unconditioned beams at different emittances are compared.

## 2.2 Soft X-ray FEL

Figure 2 shows results for nominal and twice nominal emittance, for both conditioned and unconditioned beams, in a Soft X-Ray FEL. The optimum gain length is roughly 7 m, while for an unconditioned beam the gain length is twice as long. There is some degradation of the FEL performance at higher emittance for the conditioned beam, but the performance is still much improved over the nominal, unconditioned case.

## 2.3 LCLS

Figure 3 shows the variation of FEL performance with beta function; the unconditioned beam does not improve as the focusing is made stronger, but the conditioned beam has a shorter gain length and higher saturated power for beta functions down to 4.4 m. The optimum gain length is 2.5 m, while for the unconditioned beam the gain length is 5 m.

Figure 4 shows the variation of LCLS performance with emittance; the unconditioned beam performs far worse at higher emittances, while even at 4 times nominal emittance the conditioned beam performs as well as the unconditioned beam at nominal emittance. Note that at smaller beta functions, the conditioning parameter is proportionately larger, with a value of  $23.2 \mu\text{m}^{-1}$  for a 4.4 m beta function.

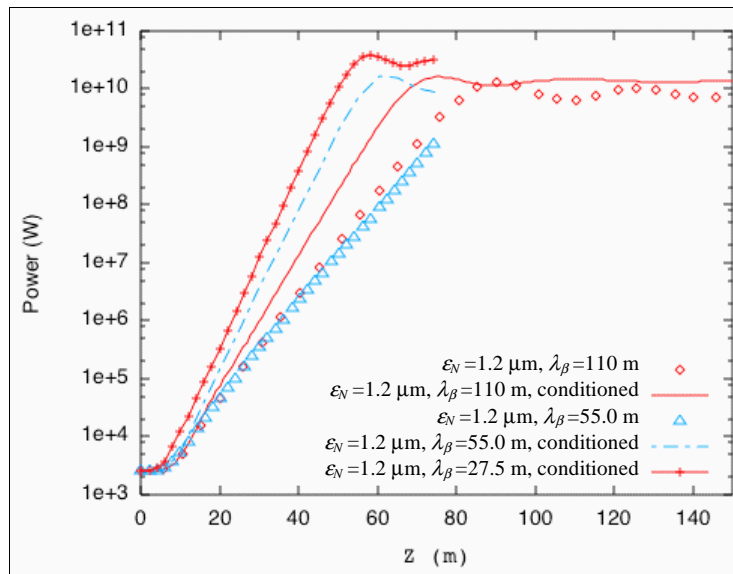
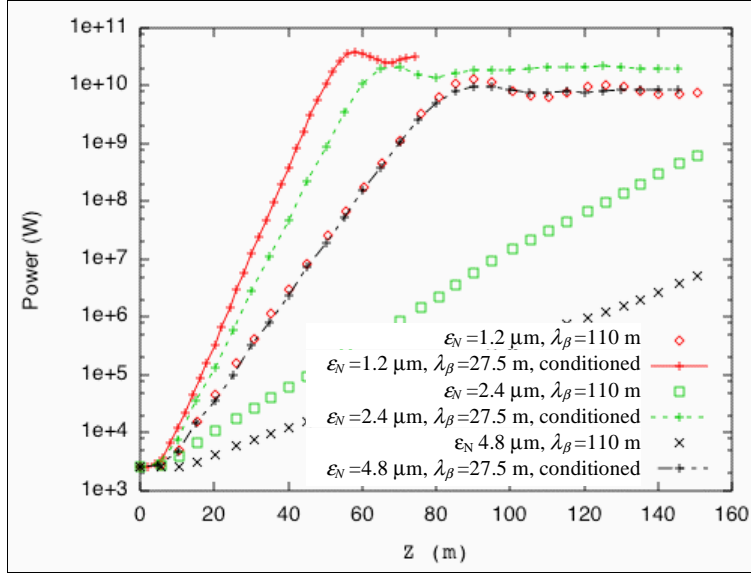


Figure 3

Radiation power as a function of undulator length for LCLS, with different beta functions, and with conditioned and unconditioned beams.



**Figure 4**

Radiation power as a function of undulator length for LCLS, with different values of beam emittance, beta function, and for conditioned and unconditioned beams. Note that a conditioned beam with four times larger emittance (black line) achieves the same performance as the nominal case (red diamonds).

## 2.4 “Greenfield” FEL

Future FELs may be imagined that reach wavelengths of  $0.1\text{\AA}$ . Using conventional design criteria this would require ultra small emittances of order  $0.1\ \mu\text{m}$ . Conditioning allows us to reach close to Greenfield FEL designs performance using a beam with an order of magnitude larger emittance and smaller beta functions.

We consider two parameter sets for Greenfield FELs (see Table 1). In both cases, FEL performance for conditioned beams improves as the betatron wavelength is reduced from the nominal design value of 110 m to 27.5 m. For the shorter betatron wavelength the conditioning parameter is  $88\ \mu\text{m}^{-1}$ . The results are shown in Figure 5 and Figure 6. At 12 GeV, for a normalized emittance of  $0.1\ \mu\text{m}$ , the gain length is 3.2 m. At emittances of  $1.2\ \mu\text{m}$ , a combination of beam conditioning and stronger focusing yields a gain length of 6 m, with a lower saturation level. At 28 GeV, for a normalized emittance of  $0.1\ \mu\text{m}$ , the gain length is 3 m. At emittances of  $1.2\ \mu\text{m}$ , a combination of beam conditioning and stronger focusing yields a gain length of 5 m, with a slightly lower saturation level.

## 2.5 Summary

Beam conditioning requires large nonlinear correlations to be introduced into the electron distribution in order to minimize the number of particles with large deviations from the resonance condition for high emittance beams. Proper conditioning then reduces sensitivity to beam emittance and allows stronger focusing in the undulator. Simulations show gain lengths a factor of two shorter, with higher saturated power, compared to unconditioned beams. The benefits of beam conditioning are seen to be applicable to a wide range of FEL designs.

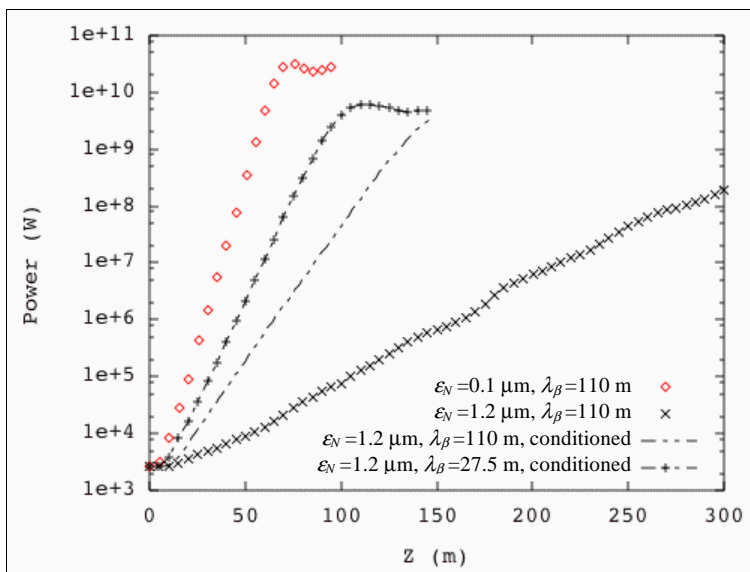


**Figure 5**

Radiation power as a function of undulator length for a “Greenfield” FEL at 12 GeV. Different betatron wavelengths and emittances are shown, with conditioned and unconditioned beams.

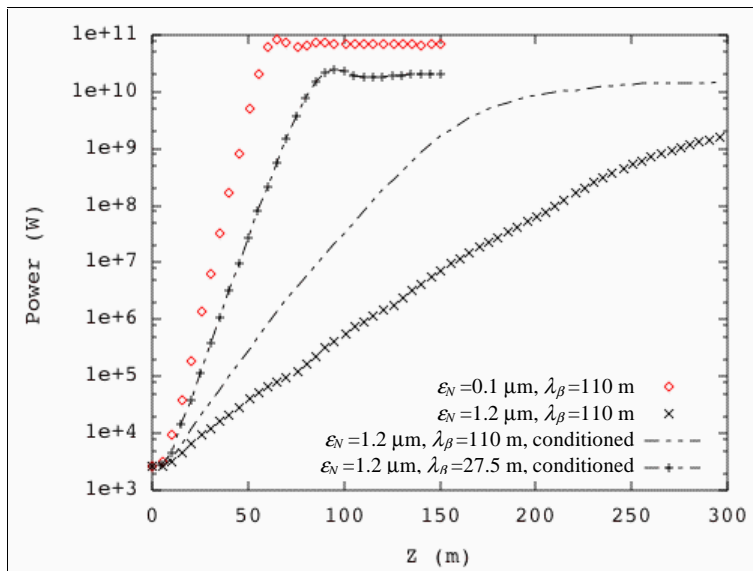


**Figure 6**

Radiation power as a function of undulator length for a “Greenfield” FEL at 28 GeV. Different betatron wavelengths and emittances are shown, with conditioned and unconditioned beams.

### 3 Beam Dynamics in Conditioning Systems

We can show in a straightforward fashion that conditioning may be achieved in a symplectic system without increase in the effective transverse emittance of the beam. For simplicity, we consider particle motion only in the longitudinal and one transverse plane; it will be seen that the extension to two transverse planes is trivial. We use canonical

action-angle variables  $(J, \phi)$  in the transverse plane, and canonical variables  $(z, \delta)$  in the longitudinal plane, with distance  $s$  along a reference trajectory as the independent variable. The reference trajectory is the path of a particle with  $J = \delta = 0$ ;  $z$  is the displacement along the reference trajectory of the selected particle with respect to a particle following the reference trajectory, and  $\delta$  is the energy deviation of the selected particle with respect to a particle following the reference trajectory.

Let us consider a system of length  $L$  defined by the integrable Hamiltonian:

$$H = \frac{\mu}{L} J + 2\pi \frac{\tilde{\xi}}{L} z J \quad (2)$$

The transformation of phase space variables following from this Hamiltonian is:

$$\begin{aligned} J_L &= J_0 & z_L &= z_0 \\ \phi_L &= \phi_0 + 2\pi \tilde{\xi} \cdot z_0 & \delta_L &= \delta_0 + 2\pi \tilde{\xi} \cdot J_0 \end{aligned}$$

The subscript 0 denotes values at  $s = 0$ , and the subscript  $L$  denotes values at  $s = L$ . Since the angle and energy deviation variables do not appear explicitly in the Hamiltonian, the action and time variables are conserved. We note that the energy deviation increases by an amount proportional to the action, so a beam of particles where the energy deviation and action are initially uncorrelated acquires a correlation between these variables:

$$\langle \delta_L J_L \rangle = 2\pi \tilde{\xi} \langle J_0^2 \rangle$$

Thus the above Hamiltonian gives the required conditioning.

We now need to consider what has been the effect on the emittance of the bunch. In terms of the Twiss parameters for a high-energy beamline, the action is defined by:

$$2J = \gamma x^2 + 2\alpha x p_x + \beta p_x^2$$

where  $x$  is the transverse co-ordinate with respect to the (dispersive) trajectory, and  $p_x$  the canonical conjugate momentum. In general, the Twiss parameters are functions of the energy deviation of the particle, but it is possible to design a beamline where the energy dependence vanishes (at least to first order) at some point in the lattice. In this case, the beam moments are correctly given by:

$$\langle x^2 \rangle = \beta \mathcal{E} \quad \langle x p_x \rangle = -\alpha \mathcal{E} \quad \langle p_x^2 \rangle = \gamma \mathcal{E} \quad (3)$$

where

$$\mathcal{E} = \langle J \rangle \quad (4)$$

is the transverse emittance of the beam, and the brackets  $\langle \rangle$  denote an average over all particles in the beam. If the action of the particles is conserved along the beamline, then the transverse emittance defined by (4) will be conserved.

It is clear from the Hamiltonian in (2) that the betatron phase advance of the particle over the conditioning system depends on its position with respect to the reference particle.

This is a benign effect from point of view of beam conditioning, but it implies that the beta function varies with longitudinal co-ordinate, since:

$$\Delta\phi = \int \frac{1}{\beta} ds$$

In practice, the beta function has an energy dependence, which is related to the chromaticity of the beamline. In a conditioner, the “required” dependence of phase advance on longitudinal co-ordinate may be associated with an energy dependence, by introducing a correlated energy spread along the bunch, as we shall see in Section 4.1. Thus, the energy dependence of the beta function may be used to give us the conditioning we require. However, there is an important point here: if the energy of the particles is changed at a location where the beta function has strong energy dependence, then the beam will become mismatched to the phase space, and an increase in effective emittance will result. These apparently conflicting requirements (for the beta function to have some variation to allow the conditioning, and to be fixed to avoid emittance growth) may be resolved by allowing the beta function to have energy dependence only at locations in the conditioner where the energy of the particles is not changing.

In summary, it appears that for a practical beam conditioner, we must satisfy two conditions:

- The action must be conserved.
- The Twiss parameters should be independent of energy at locations where the energy of the particles is changed.

The first of these conditions is easy to satisfy in a high-energy particle beamline. The second condition is more difficult. To develop some insight into how the second condition may be satisfied in practice, we first treat analytically a simple FODO-type cell. We find that the quadrupole strengths may be adjusted to cancel the first-order energy dependence of the beta function *in one plane*. To approach the condition in both transverse planes will require a more flexible beamline (i.e. more families of quadrupoles). An example of such a beamline used in a simple conditioner will be given in Section 4.1.

### 3.1 A FODO Cell Conditioner

Here we consider the energy dependence of the beta function in a simple FODO-type periodic cell, that is, one with two quadrupoles whose strengths can be adjusted independently. We look specifically at the beta function at the symmetry point, which is the center of one of the quadrupoles. For simplicity, we consider thin quadrupoles separated by a 1 m drift space; changing the length of the drift space simply rescales all the parameters in the beamline, so there are really only two free parameters, which are the strengths of the quadrupoles. Imposing the condition that the first derivative of the beta function with respect to the energy deviation vanishes uses one of the free parameters. By symmetry, the gradient of the beta function with respect to path length (in effect the Twiss alpha function) vanishes at all energies, so we only need to consider one out of the three Twiss parameters.

Considering only the horizontal plane, the transfer matrix for a thin quadrupole is:

$$Q(f) = \begin{pmatrix} 1 & 0 \\ -\frac{1}{f(1+\delta)} & 1 \end{pmatrix}$$

where  $f$  is the focal length of the quadrupole at the nominal energy. The transfer matrix for a drift space is:

$$D(L) = \begin{pmatrix} 1 & L \\ 0 & 1 \end{pmatrix}$$

The full transfer matrix for the cell is therefore:

$$M = Q\left(\frac{1}{2}f_1\right) \cdot D(1) \cdot Q(f_2) \cdot D(1) \cdot Q\left(\frac{1}{2}f_1\right) \quad (5)$$

where the focal lengths of the quadrupoles (in units of the distance between the quadrupoles) are  $f_1$  and  $f_2$ . The Twiss parameters are defined by:

$$M = \begin{pmatrix} \cos(\mu) + \alpha \sin(\mu) & \beta \sin(\mu) \\ -\gamma \sin(\mu) & \cos(\mu) - \alpha \sin(\mu) \end{pmatrix} \quad (6)$$

As we have already mentioned, symmetry ensures that  $\alpha = 0$ . Combining equations (5) and (6), we find:

$$\begin{aligned} \cos(\mu) &= \tilde{q}_1 \left(\frac{1}{2}\tilde{q}_2 - 1\right) - (\tilde{q}_2 - 1) \\ \beta \sin(\mu) &= 2 - \tilde{q}_2 \end{aligned} \quad (7)$$

where we define

$$\begin{aligned} q &\equiv \frac{1}{f} \\ \tilde{q} &\equiv \frac{q}{1+\delta} \end{aligned}$$

We expand the expression for  $\beta$  in powers of the energy deviation  $\delta$ , and impose the condition that the coefficient of the term linear in  $\delta$  is zero. This gives a relationship between the focal lengths of the quadrupoles, which, when satisfied, ensures that the first order variation in the beta function with respect to the energy deviation vanishes at the chosen symmetry point of the cell. The appropriate relationship is:

$$q_2 = \frac{1 - 2q_1 + q_1^2 \pm \sqrt{1 - 4q_1 + 4q_1^2 - q_1^3}}{\frac{1}{2}q_1^2 - q_1} \quad (8)$$

The character of the solution (for  $q_2$  and  $\beta$ ) is clearly determined by the sign of the expression  $1 - 4q_1 + 4q_1^2 - q_1^3$ . In fact, we can identify four distinct regimes, separated from each other by the roots of this expression:

$q_1 \leq \frac{3-\sqrt{5}}{2}$	$q_2$ real	$\beta$ imaginary
$\frac{3-\sqrt{5}}{2} < q_1 < 1$	$q_2$ complex	$\beta$ complex
$1 \leq q_1 \leq \frac{3+\sqrt{5}}{2}$	$q_2$ real	$\beta$ real
$\frac{3+\sqrt{5}}{2} < q_1$	$q_2$ complex	$\beta$ complex

For  $q_1 \leq \frac{3-\sqrt{5}}{2}$ , the solution is physical, but the beamline is unstable if treated as a periodic lattice. The only physical, stable solution is for  $1 \leq q_1 \leq \frac{3+\sqrt{5}}{2}$ . The nature of these solutions may perhaps be clarified if we plot the real and imaginary parts of  $q_2$  and  $\beta$  over a range of values for  $q_1$ ; these plots are shown in Figure 7.

Again, we only have a stable, physical solution for  $1 \leq q_1 \leq \frac{3+\sqrt{5}}{2}$ . That a stable physical solution is possible in only the horizontal or the vertical plane separately is seen at once by replacing  $q \rightarrow -q$ . In fact, taking the negative sign in equation (8), it is clear that the periodic beamline is unstable in at least one plane, since both quadrupoles are focusing.

It will be observed that choosing the negative sign in equation (8) gives solutions for  $q_1$  and  $\beta$  that are “better behaved”. This is emphasized if we consider the higher-order dependence of the beta function on energy. Let us take the exact solution for  $\beta$  given by equation (7), and substitute for  $q_2$  from equation (8), so as to cancel the first order dependence on energy. Then we plot  $\beta$  (normalized to the value at  $\delta = 0$ ) as a function of  $q_1$  and  $\delta$ . The results are shown in Figure 8. Apart from sensitive behavior around  $q_1 \approx 2$ , taking the negative sign in (8) ensures that the variation in  $\beta$  is less than about 0.5% over a wide range of energy error. With the positive sign in (8), the error is somewhat larger.

We have shown that with a simple periodic lattice based on a FODO-type cell, it is possible exactly to cancel the first order dependence on energy of the beta function at a symmetry point in the cell in one plane. The resulting motion is stable in the plane under consideration, but unstable in the other plane. It is not possible with such a system both to have stable motion and to cancel the energy dependence in both planes simultaneously, simply because there are insufficient free parameters to adjust to meet the conditions. In section 4.1, we give an example of a beamline using more families of quadrupoles, that *approaches* zero first order energy dependence in both planes simultaneously. However, the larger number of free parameters greatly increases the complexity of the analysis, and we have not so far performed a general study of such a system.

The dependence of the beta function on energy may be matched to zero simultaneously in both planes using a solenoid [8]. This is automatically achieved if the beta function is itself matched to the solenoid, and the solenoid acts as an  $I$  transformer (i.e. provides an identity transformation in both planes for on-energy particles). This is discussed in more detail in Section 4.2 below.

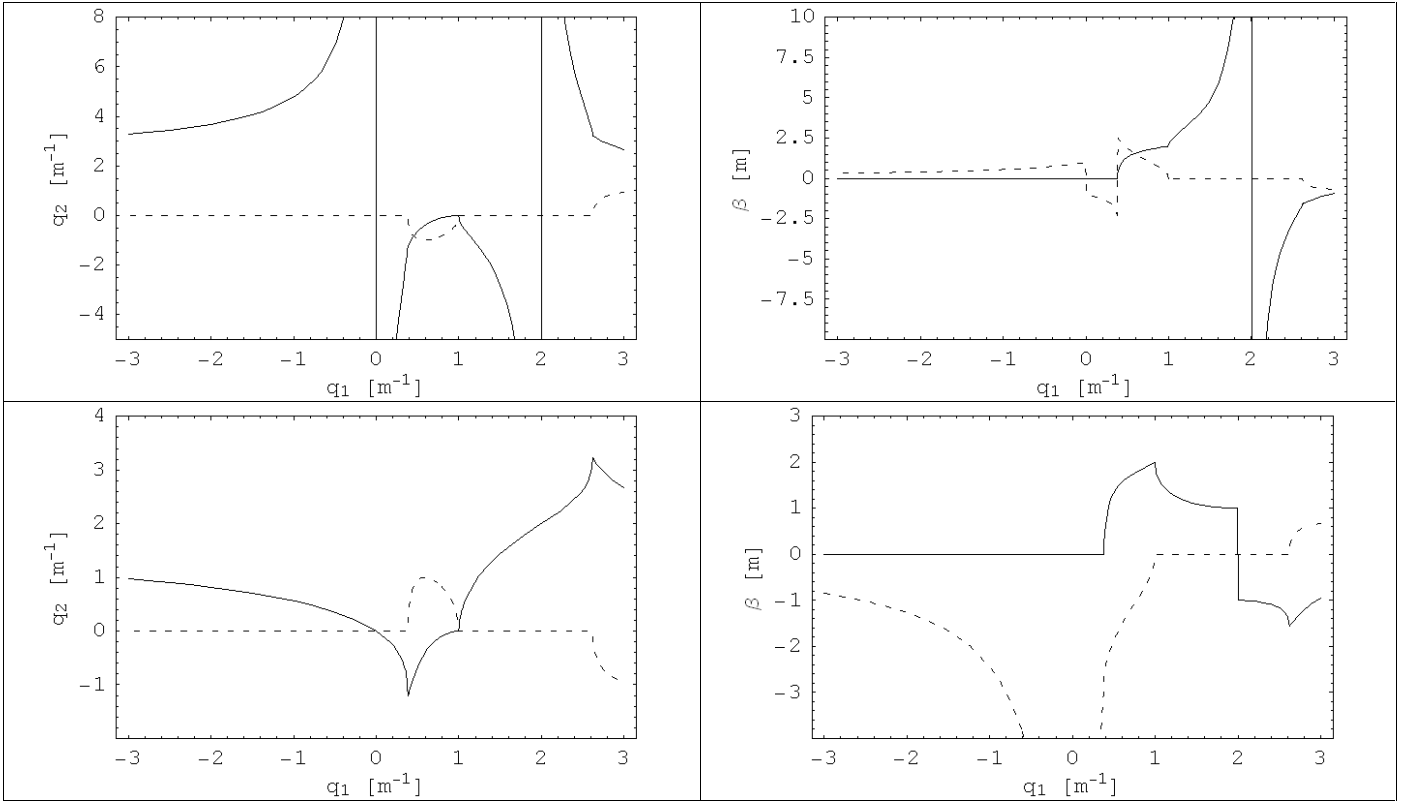


**Figure 7**

Parameters in a simple FODO-type cell with zero dependence of beta function on energy to first order at a symmetry point of the cell. Upper plots use the positive sign in equation (8), lower plots use the negative sign. Left: relationship between quadrupole strengths. Right: beta function at a symmetry point. Solid lines show the real parts and broken lines the imaginary parts.

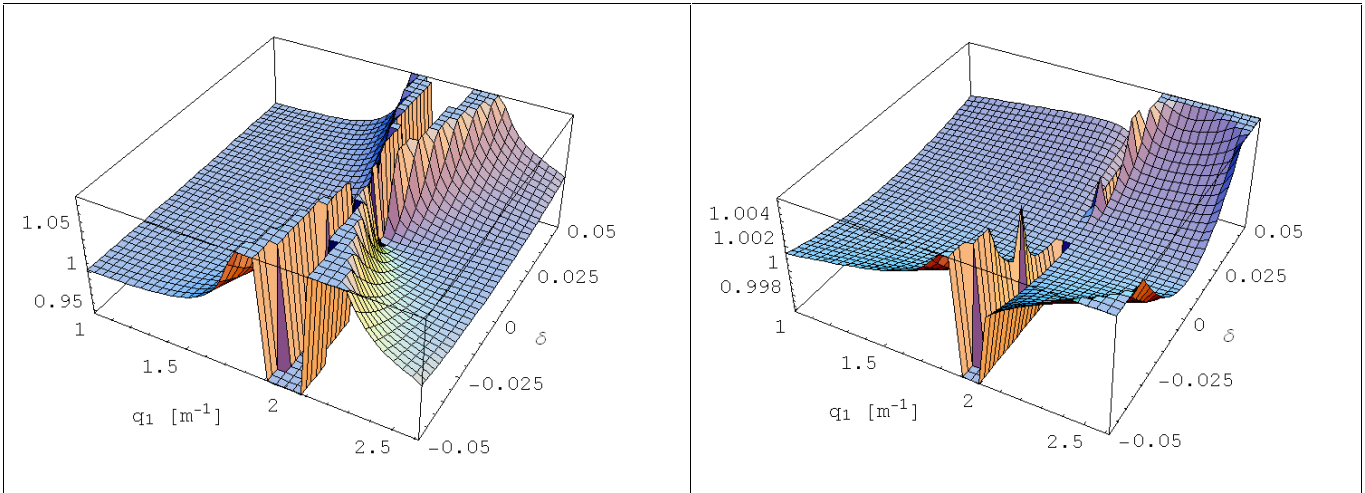


**Figure 8**

Variation in  $\beta$  as a function of  $q_1$  and  $\delta$ . Left: solution with negative sign in (8). Right: solution with positive sign in (8). The vertical axis is  $\beta/\beta_0$ , where  $\beta_0$  is the value of  $\beta$  at  $\delta=0$ . Note the different scales in the two plots.

## 4 Various Conditioners

In this section, we consider four possible realizations of conditioners that both preserve beam emittance and provide matching into the FEL along the length of the bunch.

### 4.1 A “Chromatic Conditioner”

Particle motion in a simple focusing channel may be approximately described by a Hamiltonian:

$$H = \frac{\mu}{L} J + 2\pi \frac{\xi}{L} \delta \cdot J \quad (9)$$

Here,  $\mu$  is the phase advance over the length of the beamline for a particle with the nominal energy, and  $\xi$  is the chromaticity, defined by:

$$\xi = \frac{1}{2\pi} \frac{\partial}{\partial \delta} \Delta\phi$$

where  $\Delta\phi$  is the change in angle variable of a particle over the length of the beamline. We note that the Hamiltonian (9) is essentially the same as (2) which we used in our discussion of conditioning, but with the longitudinal co-ordinate  $z$  replaced by the energy error  $\delta$ . This suggests we can construct a conditioner by first using an RF cavity to “chirp” the beam (i.e. introduce a correlation between longitudinal position and energy), then passing the beam through a focusing channel with some chromaticity, and finally using a second RF cavity to remove the chirp. The first of our conditions for a practical conditioner is satisfied by the extent to which the Hamiltonian (9) is a good approximation for the dynamics in the beamline. The second condition is satisfied if we are able to design the beamline in such a way as to make the Twiss parameters at the RF cavities independent of the particle energy. Note that it is not possible to satisfy the second condition everywhere along the beamline (since the chromaticity is related to the energy dependence of the beta function), but nor is this necessary, as we shall demonstrate.

Physically, our conditioner will work as follows. The first RF cavity effectively makes the energy deviation of particles in the bunch a linear function of the longitudinal co-ordinate. In the beamline, particles “slip back” with respect to the reference particle by a distance depending on the betatron amplitude. This is a necessary effect of the chromaticity, as is easily seen from the Hamiltonian (9). The second RF cavity “corrects” the energy deviation introduced by the first cavity. However, the energy correction will not be that required to exactly cancel the energy deviation introduced by the first cavity, and there will be a residual energy deviation depending on the particle’s betatron amplitude and the chromaticity of the beamline. This is exactly the conditioning that is required. Considering the effective emittance, if the beta functions at the RF cavities are dependent on energy, then different “slices” of the bunch will become mismatched in terms of the transverse phase space distribution. Tuning the lattice so that the beta functions are independent of energy at the cavity ensures that the bunch remains matched along its entire length going into the FEL.

As an illustration of this simple conditioner, we consider the beamline shown in Figure 9. This uses thin quadrupoles alternately focusing and defocusing as in a FODO lattice, but the quadrupoles are tuned to minimize the variation of the Twiss parameters with energy deviation at either end of the beamline, where the (thin) RF cavities are placed. In calculating the beta functions, the beamline is assumed to be periodic. In principle, the amount of beam conditioning can be increased by repeating the beamline a number of times between the two RF cavities. Figure 9 shows the beta functions in both a “matched” case, in which the quadrupole strengths are adjusted to set the energy dependence of the Twiss parameters to zero at each end of the beamline, and in a “mismatched” case, where the Twiss parameters have significant energy dependence at each end of the beamline. Figure 9 also shows the energy dependence of the beta functions; this dependence is best given in terms of the  $W$  function, which is defined by:

$$W = \sqrt{a^2 + b^2}$$

where

$$a = \frac{1}{\beta} \frac{\partial \beta}{\partial \delta} \quad b = \frac{\partial \alpha}{\partial \delta} - \frac{\alpha}{\beta} \frac{\partial \beta}{\partial \delta}$$

To understand the significance of the  $W$  function, note that at a symmetry point in a beamline (as at either end of the focusing channel shown in Figure 9) the symmetry condition enforces  $\alpha = 0$  at all energies, and we have then simply:

$$\frac{\Delta \beta}{\beta} \approx W \cdot \delta$$

In other words, the fractional change in the beta function is just  $W$  times the energy deviation.

In the matched case, the values of the  $W$  functions at the start and end of the beamline are essentially zero. In between, the non-zero values indicate variation in the beta functions (and hence the phase advance) with energy, which is a necessary feature for the conditioning. In fact, the larger the values of the  $W$  functions, the more conditioning is provided. Note that the required tuning of the quadrupoles may be achieved easily in a lattice design code such as MAD [9].

Let us consider the results of tracking through a beamline constructed from 60 repetitions of the cell shown in Figure 9, with RF cavities at either end to apply and cancel an energy chirp. To begin with, we consider the matched case. Figure 10 shows the energy deviation of a collection of particles as a function of horizontal co-ordinate before and after tracking the beamline. The particles are arranged in five groups, each group having a different horizontal action up to  $5.3 \mu\text{m}$ , and a different initial longitudinal co-ordinate ranging from  $-2 \text{ mm}$  to  $+2 \text{ mm}$ . The initial energy chirp gives the particles an energy deviation proportional to the longitudinal co-ordinate. The energy deviation of each particle before the initial energy chirp is zero. At the end of the beamline, we see that the energy deviation of each particle is related (actually proportional) to the action, so the conditioning has been achieved as desired. Figure 11 shows the horizontal phase space of

the particles before and after tracking. There is no visible distortion of the phase space ellipses, and the change in the effective emittance is negligible.

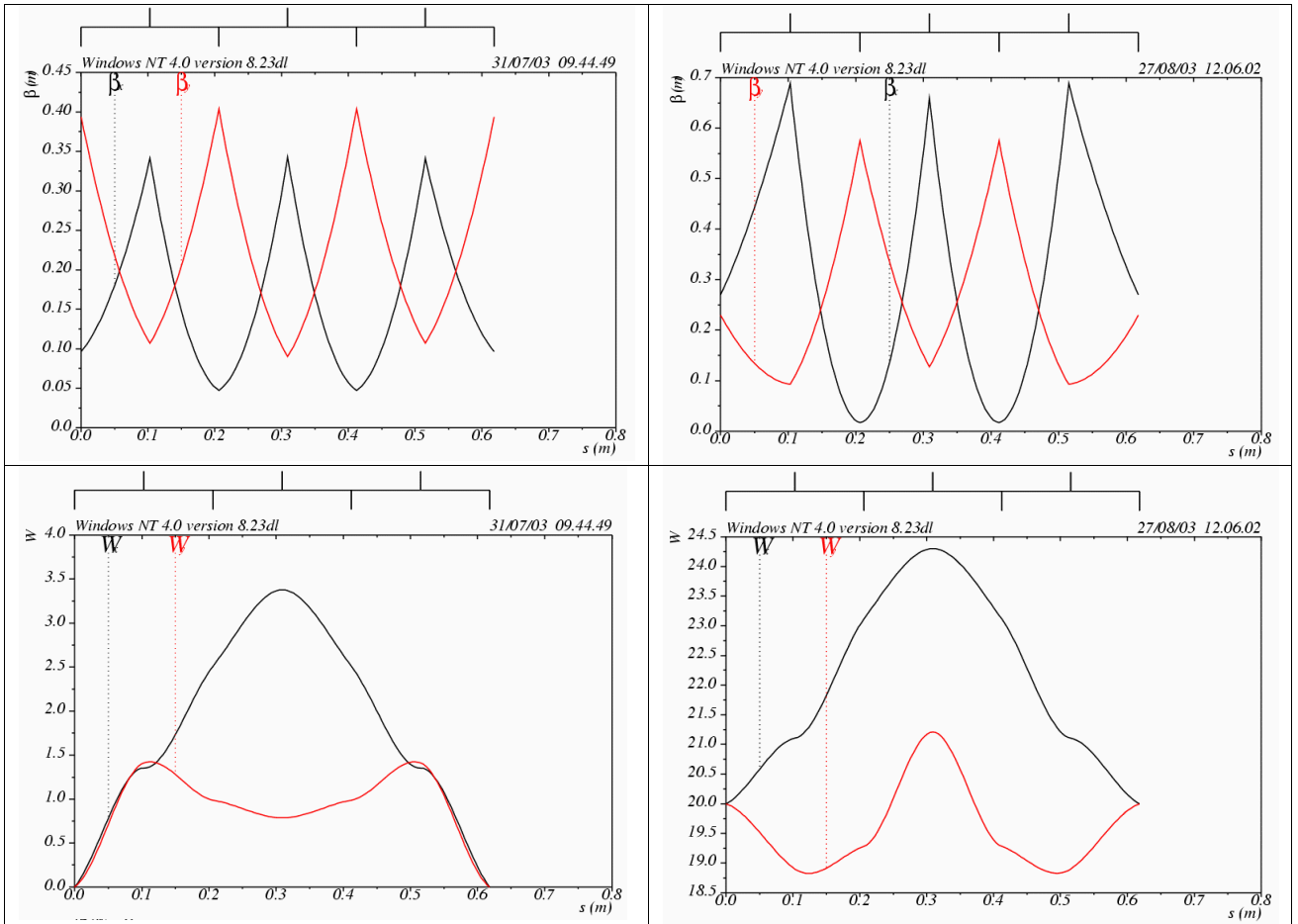


**Figure 9**

(Top) Beta functions in a simple conditioning chromatic beamline. The left-hand plot shows the “matched” case, and the right-hand plot the “mismatched” case. (Bottom) Energy dependence of the beta functions for the same “matched” and “mismatched” cases, given in terms of the  $W$  functions.

Now let us consider the mismatched case, in which the strengths of the quadrupoles are adjusted to give the Twiss parameters some significant energy dependence at either end of the beamline. The results of tracking through this beamline are shown in Figure 12 and Figure 13.

First, we notice that there is now a significant dependence of the change in energy deviation on the initial angle of the particle, as well as on the action (this is clear from the variation from a straight line in the plot for each group of particles with a given action). We also notice that the amount of conditioning is about a factor of three larger than in the conditioned case; this is expected from the larger values of the  $W$  function in the mismatched case compared to the matched case. Finally, we notice that the shapes of the ellipses in the horizontal phase space have been changed as a result of passing through

the conditioner; this is consistent with the change in the Twiss parameters with the different energies of the different groups of particles.

Unfortunately, the amount of conditioning that may be provided by this simple chromatic conditioner with realistic parameters is not great. The parameters of the matched example are given in Table 2.

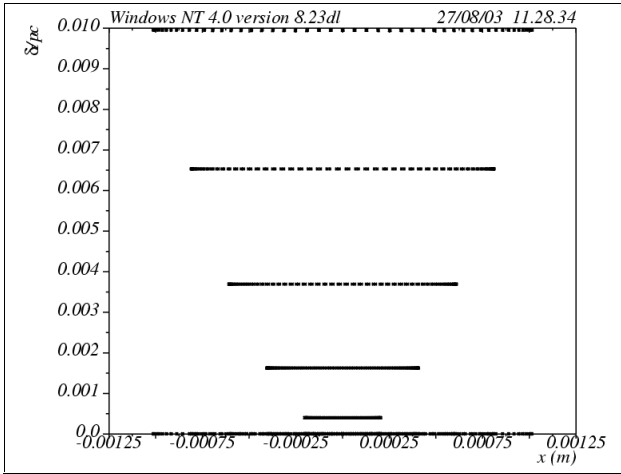


**Figure 10**

Energy vs horizontal co-ordinate after tracking through the matched conditioner.

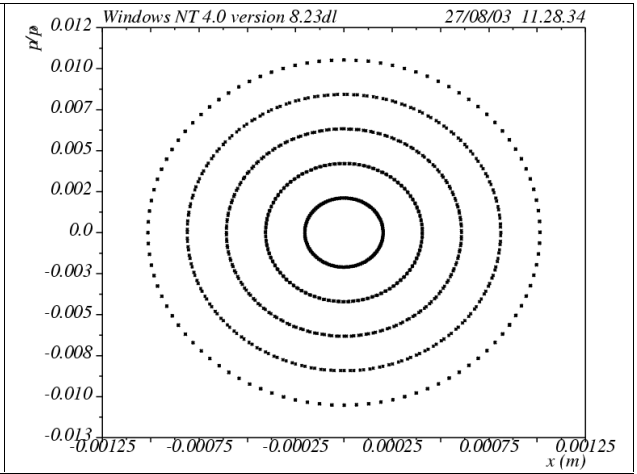


**Figure 11**

Horizontal phase space before and after tracking through the matched conditioner.

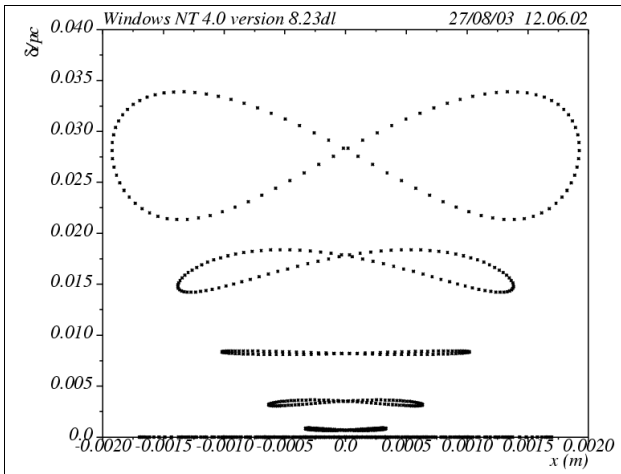


**Figure 12**

Energy vs horizontal co-ordinate after tracking through the mismatched conditioner.

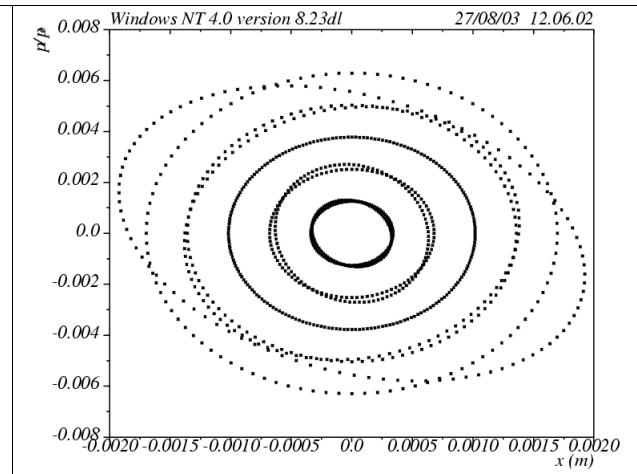


**Figure 13**

Horizontal phase space before and after tracking through the mismatched conditioner.

**Table 2**

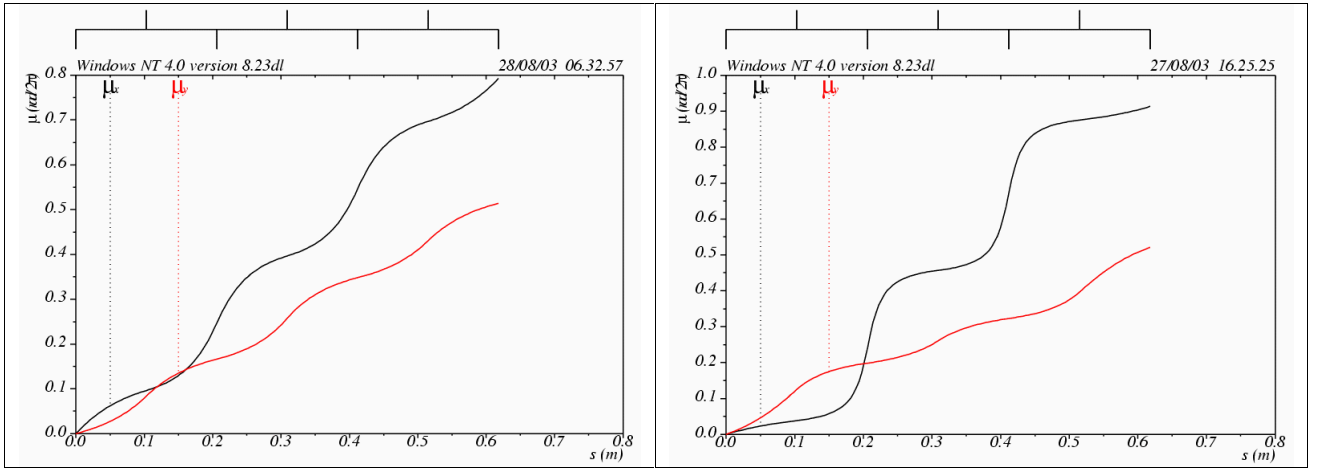
Parameters in the example matched chromatic conditioning beamline.

Beam Energy	$E$	1 GeV
Normalized emittance	$\langle \gamma \mathcal{J} \rangle$	5.34 $\mu\text{m}$
RF Voltage	$V_{RF}$	52.4 MV
RF Frequency	$\omega_{RF}$	$2\pi \times 4.85$ GHz
Max Quad Strength	$k_1 l$	15.2 $\text{m}^{-1}$
Beamline Length	$L$	37 m
Chromaticity	$\xi$	-57.4
Conditioning	$\Delta\gamma/\gamma \mathcal{J}$	0.0019 $\mu\text{m}^{-1}$

Note that from the Hamiltonian (9), we find that the amount of conditioning in a chromatic conditioner is given by:

$$\frac{\Delta\gamma}{\gamma \mathcal{J}} = -2\pi \frac{eV_{RF}}{E} \frac{\omega_{RF}}{c} \xi$$

Using the parameters in Table 2, we find that the change in energy deviation for a particle with action 5.34  $\mu\text{m}$  is about 0.01, in good agreement with the tracking results shown in Figure 10. The amount of conditioning provided by this beamline is  $1.9 \times 10^{-3} \mu\text{m}^{-1}$ , or about 3000 times smaller than that required, for example, by LCLS.

**Figure 14**

Betatron phase advances across the matched (left) and mismatched (right) chromatic conditioning cell.

It is worth considering briefly the dependence of the conditioning on betatron phase that is apparent in the mismatched conditioner (Figure 12). Our Hamiltonian in (9) averaged the phase advance over the length of the beamline. In a finite beamline, this is not necessarily a good approximation: physically, the length of the trajectory of a particle through the conditioning cell depends not just on the betatron amplitude, but also on the betatron phase. Figure 14 shows the betatron phase advance over one cell of the chromatic conditioner. In the case where the  $W$  functions are properly matched to zero at either end of the beamline, the phase advance is significantly “smoother” than in the

mismatched case. This is not necessarily a direct consequence of the behavior of the  $W$  functions, but rather of the beta functions. Over a number of cells, the dependence of the length of the trajectory of a particle on the initial betatron phase can be averaged out or not, depending on the exact number of cells. For 60 cells, which we used in the conditioning example in this section, the phase dependence in the matched cell clearly averages out, since in Figure 10 the final energy deviation depends only on the betatron amplitude, and there is negligible dependence on phase.

## 4.2 A Solenoid-based Conditioner

Instead of using quadrupoles to focus the beam as in the simple chromatic conditioner, we can use a solenoid as proposed in Reference [2]. The importance of matching the beam to the solenoid was observed by Kim [8]. The basic arrangement and principles of operation are the same as for the chromatic conditioner: a solenoid is “sandwiched” between two RF cavities, with the cavities tuned to apply an energy chirp at the entrance to the solenoid, and cancel the chirp at the exit. In general, a particle follows a helical path through the solenoid, with the radius of the path determined by the horizontal and vertical co-ordinates of the particle at the entrance of the solenoid. For simplicity, let us consider a solenoid of length  $L$  that is tuned such that the linear transfer matrix in the two transverse planes is the identity, i.e.

$$|k|L = 2n\pi$$

where  $n$  is an integer, and

$$k = \frac{B_z}{B\rho}$$

$B_z$  is the longitudinal solenoid field, and  $B\rho$  is the beam rigidity. To match the beam to the solenoid, we need to impose the condition:

$$\beta = \frac{1}{k}$$

In this case, it turns out that the chromatic variation in the beta function is zero, as well as the beta functions being constant along the length of the solenoid. The change in longitudinal co-ordinate from a particle passing through a single solenoid is given by:

$$\Delta z_1 = -\frac{1}{2}k^2L\beta(J_x \cos^2(\phi_x) + J_y \cos^2(\phi_y))$$

If we consider two solenoids separated by a  $\pi/2$  betatron phase advance in both planes, then the combined change in longitudinal co-ordinate is:

$$\Delta z = -\frac{1}{2}k^2L\beta(J_x + J_y)$$

Now adding an RF cavity to chirp the beam at the entrance to the first solenoid, and a second RF cavity to “cancel” the chirp (in the case of zero betatron amplitude) at the exit of the second cavity, we find the following expression for the amount of conditioning provided:

$$\frac{\Delta\gamma}{\gamma J} = \frac{eV_{RF}}{E} \frac{\omega_{RF}}{c} \frac{B_z L}{4B\rho} = \frac{eV_{RF}}{E} \frac{\omega_{RF}}{c} \frac{n\pi}{2}$$

where  $J = J_x + J_y$ . Although it is possible, in principle, to increase the amount of conditioning by using a large beta function, if the beta function is not properly matched to the solenoid, then there can be a strong dependence of the Twiss parameters on the energy deviation, and a growth in the projected transverse emittance.

As an example, we consider the parameters given in Table 3. Note that  $B_z L/B\rho = 2\pi$  in this example. These parameters give a conditioning of roughly  $1.6 \times 10^{-6} \mu\text{m}^{-1}$ , which is about 6 orders of magnitude small than the amount of conditioning needed for the examples given in Section 2.

**Table 3**

Parameters for estimate of conditioning provided by a solenoid conditioner.

Beam energy	$E$	1 GeV
RF Voltage	$V_{RF}$	10 MV
Cavity frequency	$\omega_{RF}$	$2\pi \times 4.85$ GHz
Integrated solenoid field	$B_z L$	20.96 Tm

### 4.3 A $\text{TM}_{210}$ Cavity Conditioner

Sessler, Whittum and Yu [1] have suggested using an RF cavity operating in the  $\text{TM}_{210}$  modes, and already realized the varying phase space mismatch that can occur along the length of a bunch with non-zero length. This mismatch may be avoided using the techniques described above, to eliminate the (first-order) dependence of the beta function on energy. The amount of conditioning provided by a conditioner based on a  $\text{TM}_{210}$  cavity may be written:

$$\frac{\Delta\gamma}{\gamma J} = \frac{1}{\gamma} \frac{eE_0}{mc^2} \frac{\omega_{RF}}{c} \beta$$

where  $E_0$  specifies the peak longitudinal electric field in the cavity [10]:

$$E_z = \frac{1}{4} \left( \frac{j_{21}}{R} \right)^2 (x^2 - y^2) E_0 \cos(\omega_{RF} t)$$

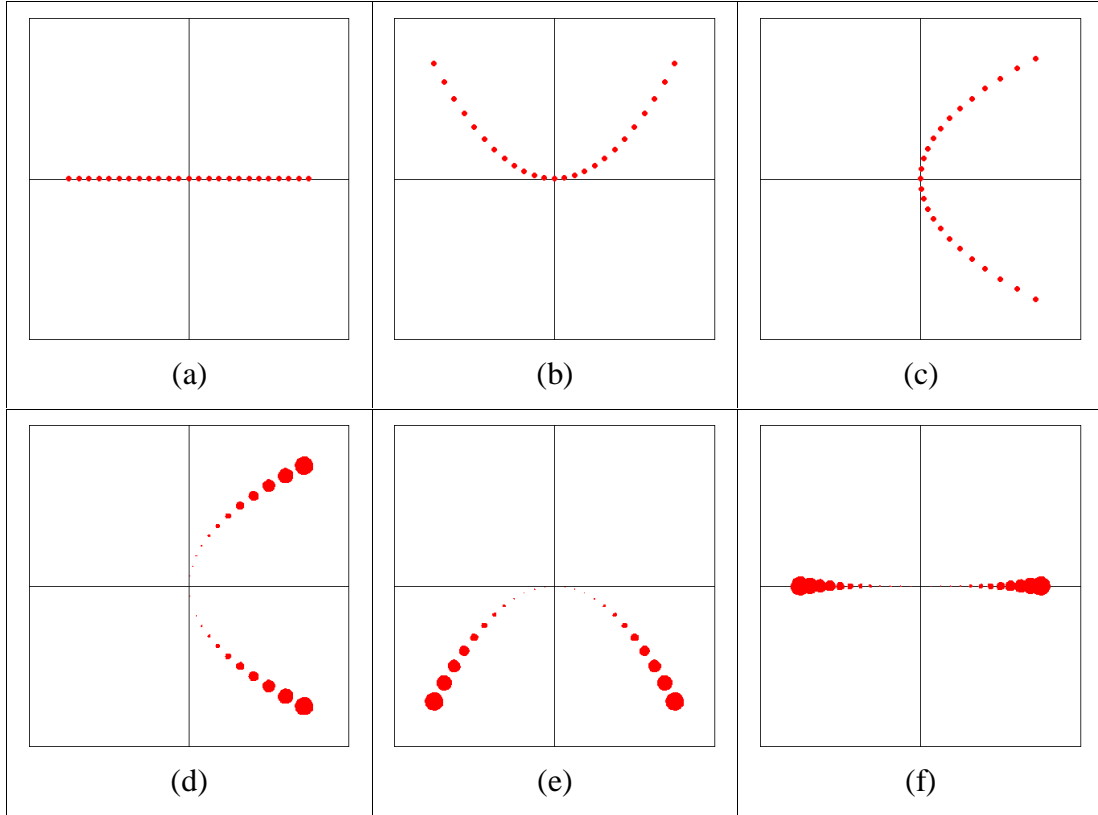
for cavity radius  $R$  and frequency  $\omega_{RF}$ .  $j_{21}$  is the first zero of the Bessel function  $J_2$ . As an example, we consider the parameters given in Table 4. These parameters give a conditioning of roughly  $10 \times 10^{-6} \mu\text{m}^{-1}$ , which is again small compared to the amount of conditioning needed for the examples given in Section 2.

**Table 4**Parameters for estimate of conditioning provided by  $TM_{210}$  cavity conditioner.

Beam energy	$E$	1 GeV
Cavity field amplitude	$eE_0/mc^2$	$10 \text{ m}^{-1}$
RF Power		1 MW
Cavity frequency	$\omega_{RF}$	$2\pi \times 4.85 \text{ GHz}$
Beta function	$\beta$	20 m

**4.4 A  $TM_{110}$  Cavity Conditioner**

The use of a cavity operating in  $TM_{110}$  mode for beam conditioning has previously been discussed [1,10]. Here, we extend the conditioner to a bunch with non-zero length by using such a cavity together with sextupoles used temporarily to distort the transverse phase space. In particular, the beamline is simply a  $TM_{110}$  mode cavity in between two sextupoles, with simple  $90^\circ$  FODO cells separating each sextupole from the cavity. Physically, the way this system works is straightforward (see Figure 15).

**Figure 15**

Horizontal phase space transformations through the sextupole- $TM_{110}$  cavity. (a) Initial distribution of particles. (b) After passing through first sextupole. (c) After first  $90^\circ$  FODO cell. (d) After passing through  $TM_{110}$  cavity. The size of the point indicates the energy of the particle. (e) After passing through second FODO cell. (f) After passing through second sextupole.

The first sextupole introduces a correlation between  $p_x$  and  $x^2$ . The first FODO cell rotates the phase space so that this becomes a correlation between  $x$  and  $p_x^2$ . In other words, the phase space is now asymmetric in  $x$ , with particles with larger betatron

amplitudes being further to one side of the beam. These particles are accelerated in the RF cavity, which has a longitudinal electric field varying linearly with  $x$ . The second FODO cell simply rotates the phase space once more, so the second sextupole then cancels the phase space distortion introduced by the first sextupole.

This system offers the potential for stronger conditioning than the previous systems considered, since it is straightforward to achieve large phase space distortions using sextupoles of even moderate strength. If it were not for the chromatic effects in the FODO cells, it would be possible to produce sufficient conditioning for LCLS, for example, in just a few passes of the conditioner. However, the different energies of particles in the beam means that different particles undergo phase space rotations through different angles, and the second sextupole does not exactly cancel the distortion introduced by the first. This will lead to large growth of the projected emittance. To avoid this growth, it is necessary to limit the amount of distortion provided by the first sextupole.

To study this system in a little more detail, we can consider simplified lowest-order maps for the individual sections. For the sextupoles at the entrance and exit of the conditioner, our map is:

$$x_f = x_i$$

$$p_{x,f} = p_{x,i} + \frac{k_2 l}{2(1 + \delta)} x^2$$

For the FODO cell, the map is:

$$\begin{pmatrix} x \\ p_x \end{pmatrix}_f = \begin{pmatrix} \cos(\tilde{\mu}) & \beta \sin(\tilde{\mu}) \\ -\frac{1}{\beta} \sin(\tilde{\mu}) & \cos(\tilde{\mu}) \end{pmatrix} \begin{pmatrix} x \\ p_x \end{pmatrix}_i$$

where

$$\tilde{\mu} = \frac{\pi}{2} + 2\pi\xi \cdot \delta$$

for chromaticity  $\xi$ . Note that for a simple FODO cell with  $90^\circ$  phase advance, the chromaticity is (in the thin lens approximation):

$$\xi = -\frac{1}{\pi} \tan\left(\frac{\mu}{2}\right) = -\frac{1}{\pi}$$

For the  $TM_{110}$  cavity, the map is [10]:

$$\begin{aligned}x_f &= x_i + p_x L - \frac{2}{\gamma} \left( \frac{c}{\omega} \right)^2 \frac{eB}{mc} [\sin(\theta)\sin(\psi) + \theta \sin(\psi - \theta)] \\p_{x,f} &= p_{x,i} + \frac{2}{\gamma} \frac{c}{\omega} \frac{eB}{mc} \sin(\theta)\cos(\psi) \\\delta_f &= \delta_i + \frac{2}{\gamma} \frac{eB}{mc} x_i \sin(\theta)\sin(\psi)\end{aligned}$$

where

$$\theta = \frac{\omega L}{2c} \quad \psi = \frac{\omega}{c} z + \theta$$

and

$$\gamma = \gamma_0(1 + \delta_i)$$

This map includes (through the “phase” angle  $\psi$ ) the  $z$ -dependent kick that comes from the magnetic field in the cavity.

To understand how this system conditions the beam, let us consider the case of particles with  $z = \delta = 0$ , and take  $\theta = 3\pi/2$ . Let  $J$  be the initial action and  $\phi$  be the initial angle (betatron phase) of one of the particles. Then it is straightforward to show that at the entrance to the cavity, the horizontal co-ordinate is:

$$x = \sqrt{2\beta J} \sin(\phi) + k_2 l \beta^2 J \cos^2(\phi)$$

Then the change in energy deviation is:

$$\Delta\delta = \frac{2}{\gamma} \frac{eB_0}{mc} \left[ \sqrt{2\beta J} \sin(\phi) + k_2 l \beta^2 J \cos^2(\phi) \right]$$

Now suppose we make  $N$  passes through the whole system, starting from a different betatron phase each time, so we can average over all values of  $\phi$ . The total change in energy deviation is:

$$\Delta\delta_N = \frac{N}{\gamma} \frac{eB_0}{mc} k_2 l \beta^2 J$$

and hence:

$$N \left\langle \frac{\Delta\gamma}{\gamma J} \right\rangle = \frac{N}{\gamma} \frac{eB_0}{mc} k_2 l \beta^2 \quad (10)$$

This is written in terms of an “average conditioning per pass”, although it is important to remember that conditioning is only properly obtained in this system by making many passes through the system.

The effects of the longitudinal distribution of particles (in  $z$  and  $\delta$ ) are not necessarily small. To estimate the impact, we can simulate the conditioner, by applying the above maps in the appropriate sequence some number of times to an artificial distribution. The distribution we choose has the following properties:

- The action  $J$  is the same for all particles.
- The angle variables  $\phi$  are uniformly distributed round the phase space ellipse.
- The distribution of longitudinal co-ordinate  $z$  is Gaussian with mean 0 and rms  $\sigma_z$ .
- The energy deviation of all particles is initially zero.

The parameters we choose for the simulation are given in Table 5. In addition we choose the betatron phase advance between passes through the conditioner to be  $0.25 \times 2\pi$ . Selecting a phase advance close to a quarter integer helps to minimize the effect of the transverse kick from the magnetic field in the cavity. Note that in the case of the simple chromatic conditioner and the solenoid conditioner, we imposed a specific condition on the chromatic effects (specifically, on the  $W$  functions) to avoid any growth in the transverse emittance. In the present case, we are not imposing such a condition, but are relying on the chromatic effects being small in each individual pass, and *not* adding coherently over many passes through the system.

**Table 5**

Parameters for simulation of  $\text{TM}_{110}$  cavity conditioner.

Normalized action	$\gamma J$	4.8 $\mu\text{m}$
Beam energy	$E$	2 GeV
Bunch length	$\sigma_z$	200 $\mu\text{m}$
Sextupole strength	$k_2 l$	360 $\text{m}^{-2}$
Cavity field amplitude	$eB_0/mc$	20 $\text{m}^{-1}$
Beta function	$\beta$	20 m

The results of the simulation for 4000 passes of a beam of 200 particles through the conditioner are shown in Figure 10. Although the conditioning has introduced some scatter into the horizontal phase space, the particles all lie close to the original ellipse: the mean action has increased by 10%. The change in the energy corresponds to a total conditioning (taking the mean of  $\Delta\gamma/\gamma J$  over all particles in the bunch) of  $2.9 \mu\text{m}^{-1}$ , in agreement with the value expected from equation (10).

The normalized action we used in the simulation is four times the specification for LCLS, and is a value that should be readily achievable with an RF photocathode gun. With this emittance, the same FEL performance can be achieved as for the nominal parameters (Table 1) if the beta function in the undulator is reduced to 4.4 m, and the beam is conditioned (see Figure 4). The necessary conditioning parameter is  $\kappa_x = 23.2 \mu\text{m}^{-1}$ . Thus the conditioning provided in our simulation is roughly one eighth of that needed for LCLS with  $4.8 \mu\text{m}$  emittance; however, the bunch length is also eight times longer than the final bunch length, and an appropriate bunch compressor can amplify the conditioning by the necessary factor of eight<sup>1</sup>.

<sup>1</sup> Conservation of the longitudinal emittance requires that any reduction of bunch length be accompanied by a corresponding increase in energy spread.

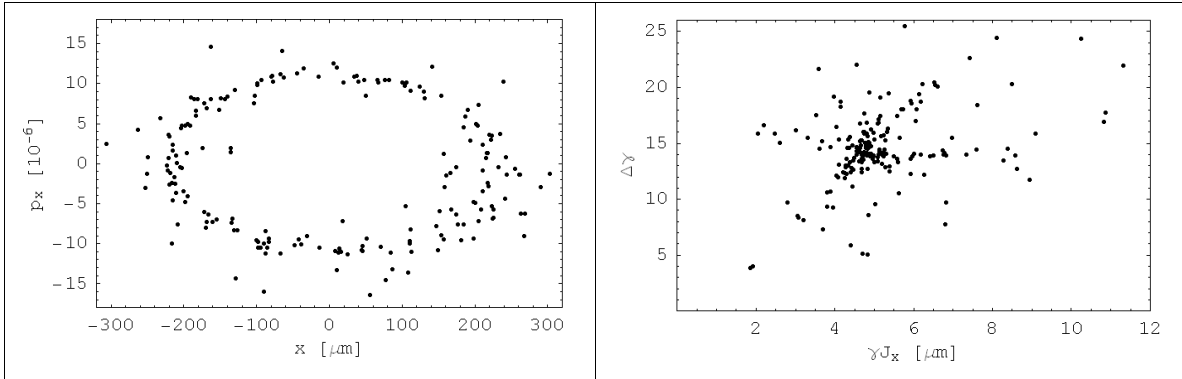


**Figure 16**

Results of simulation of  $TM_{110}$  cavity conditioner. Left: horizontal phase space after conditioning. Right: correlation between energy error and horizontal action after conditioning. Initially, all particles in the beam have normalized horizontal action  $4.8 \mu\text{m}$ , gaussian longitudinal distribution with rms  $200 \mu\text{m}$ , and no energy error. After conditioning, the horizontal emittance has increased 10%, and the rms energy spread is 0.1%.

#### 4.5 A “Conditioning Ring”

The conditioning schemes we have discussed in this section each require many thousands of passes to provide the level of conditioning required for contemporary FELs. Including a conditioner as an insertion in a ring might offer a path to making these conditioners practical. A conditioning ring is shown in concept in Figure 17.

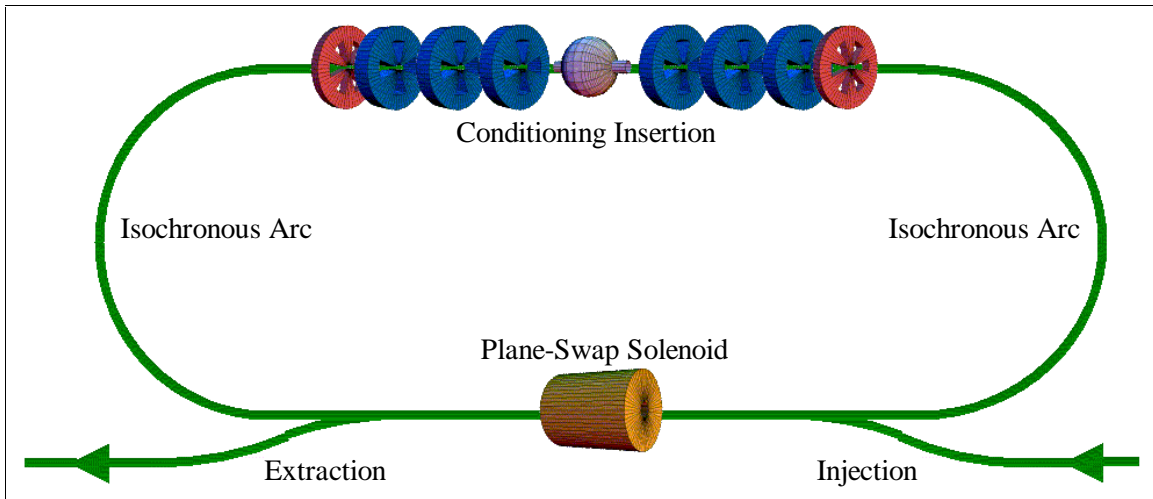


**Figure 17**

Conceptual layout of a conditioning ring. The conditioner in this case is that described in section 4.4, consisting of a  $TM_{110}$  mode cavity, separated on either side by  $90^\circ$  FODO cells from sextupole magnets. The plane-swap solenoid allows conditioning in horizontal and vertical planes on alternate passes through the conditioning insertion.

It will likely be difficult in practice to realize a conditioning ring. To avoid synchrotron radiation effects, the ring would need to be operated at low energy with weak bending magnets, and the beam stored for the minimum number of turns. Even a few thousand

turns could be too many, and it will be necessary to use a very effective conditioning scheme in the insertion. The low energy will make the beam vulnerable to a variety of collective effects, particularly since the bunches will tend to be short, with high peak currents. Design and tuning of the arcs will be important, since any phase slip will affect the longitudinal structure of the bunch. The main advantage of the conditioning ring lies in the fact that the conditioning system can be made relatively compact, compared to the otherwise very long beamline that would be needed.

## 5 Laser and Laser-Plasma Conditioners

Laser Compton back-scattering and laser-plasma wake field acceleration provide two possible mechanisms for conditioning beams. Here, we briefly describe the methods and the advantages and difficulties associated with each method.

### 5.1 Laser Back-Scattering

A laser beam fired into a beam of electrons will undergo some back-scattering, the amount of scattering, from any one electron, is given by the flux of photons ( $\# / \text{cm}^2 \text{sec}$ ), the length of laser pulse (sec), and the Compton cross section ( $\text{cm}^2$ ). In this process a photon of energy  $h\nu$  will be up-shifted in energy by amount  $4\gamma^2$ .

For conditioning we need to shape (radially) the laser pulse, which can easily be done, as the beam radial size is large compared to the laser light wavelength. In addition, we must also do the scattering process at low electron energy so that the electron's energy is not changed too much in one collision. In fact, since different electrons will experience different numbers of scatters we need to have the average number of scatters from any one electron large (perhaps 100 scatters), so that the spread in number is relatively small and, therefore, acceptable.

Putting these ideas together, we find that conditioning at 50 MeV (above the energy where space charge is important), and producing 5 MeV of conditioning, with 1 micron photons, and a pulse length of 10 picosec, would require a total laser energy of a few hundred joules. The intensity of light is low enough that non-linear processes do not occur. The conditioning must be spread out over a number of different betatron phases, which would, at the same time, reduce the laser requirement at any one section.

The Compton scattering will, also, lead to emittance growth, as the scattered photon will not be strictly forward, but typically within the angle  $1/\gamma$ . The emittance growth is proportional to the electron beam radius and varies inversely with  $\gamma$ . Focusing the electron beam at the interaction point is needed to reduce the emittance growth to an acceptable amount.

Independent work on the laser back-scattering method may be found in Ref [11].

### 5.2 Laser-Plasma Wake Field Acceleration

A laser pulse going through a plasma will produce a wake and this wake, acting on an electron bunch just following the laser pulse, can be employed to condition the bunch. In order to have a radial variation of the longitudinal wake the laser pulse needs to be shaped (radially) and the plasma density chosen so that one is in the linear regime. The

wake is most efficiently generated when the laser pulse length is equal to the plasma oscillation wavelength.

Possible parameters are a laser of wavelength 1 micron, pulse length of 0.3 picosec, energy per pulse of 0.3 J, plasma density of  $2 \times 10^{16} \text{ cm}^{-3}$ , plasma length 0.6 cm. Acting on an electron pulse of radius 30 microns this would produce 5 MeV of conditioning; i.e., a difference between the center and the radial edge of the beam of 5 MeV of energy gain (or loss). Twice the Rayleigh length is 0.6 cm, which is consistent with the length of the plasma.

The radial focusing field is strong, of the order of 20% of the peak accelerating field, but presumably this can be handled by the methods described in previous sections. Non-linearity of the radial field can be controlled by proper shaping of the laser pulse.

Scattering of the electrons by the plasma will lead to emittance growth, but the effect is small.

### 5.3 Comments

The Compton method requires a powerful laser and it must be done at low energy so the conditioning needs to be preserved through the acceleration process. The emittance growth is acceptable, but requires a focus at the interaction point. The physics of the Compton method is straightforward.

The wake-field method can be done at high energy and does not require a very powerful laser. The method requires a lattice for handling the radial kicks. The method requires a good understanding, and control, of plasma behavior.

## 6 Conclusions

We have shown that beam conditioning in free-electron lasers allows for operation at significantly larger emittances than are envisioned for soft X-ray FELs, the LCLS and the so-called Greenfield X-ray FEL sources. Previously perceived limitations to conditioning, based on an assumption that conditioning introduces a mismatch in the transverse phase space dependent on longitudinal position in the bunch, are readily avoided by a proper design of the conditioner. We demonstrate that the proper design of a conditioner requires that (a) the conditioning correlate energy with transverse action, and that (b) the beamline Twiss parameters be independent of energy at points of the conditioner where the particle energy is changed. Under these conditions there is no increase in the effective emittance. We have three realizations of conditioning lattices using conventional technology, based on solenoids, quadrupoles, and sextupoles. Conditioning at low energy is easier, but requires that the conditioning be preserved throughout the subsequent acceleration and transport. Conditioning at high-energy requires a long conditioner section, leading us to propose a conditioning ring. The possibility of conditioners based on plasma wakefields or laser Thompson scattering is briefly examined.

Finally, there is much work to be done. Conditioning rings need to be further explored, including radiation and collective effects; Greenfield FELs may benefit from an

acceleration scheme that has conditioning sections built into it so that the beam emerges already conditioned. Laser and laser-plasma systems have only begun to be explored.

## 7 Acknowledgements

We should like to thank P. Emma, E. Esarey, W. Fawley, K.-J. Kim, and G. Stupakov for useful discussions. The method described in Section 5.1 has been independently arrived at, and evaluated, by C. Schroeder, E. Esarey and W. Leemans.

## References

- 
- [1] A. M. Sessler, D. H. Whittum and L.-H. Yu, "Radio-Frequency Beam Conditioner for Fast-Wave Free-Electron Generators of Coherent Radiation", Phys. Rev. Lett. 68, 3, pp.309-312, 1992.
  - [2] G. Stupakov and P. Emma, Phys. Rev. ST AB, Volume 6, 030701 (2003).
  - [3] S. Reiche, Nucl. Instr. Meth. A 429, p. 243 (1999).
  - [4] R. Carr et al, "The VISA FEL Undulator", Proceedings of the 20th International FEL Conference (FEL98), Williamsburg, VA, August 1998.
  - [5] Built upon LUX: J.N. Corlett et al, "Feasibility study for a recirculating linac-based facility for femtosecond dynamics", Lawrence Berkeley National Laboratory Report LBNL-51766 (2002).
  - [6] The LCLS Design Study Group, LCLS Design Study Report, SLAC-R-521 (1998).
  - [7] J. Galayda, K.-J. Kim, J. Murphy, "High Brightness Electron Beams for X-Ray FELs", Proceedings of COOL03 Workshop on Beam Cooling and Related Topics, Lake Yamanaka, Japan, 2003. To be published in Nuclear Instruments and Methods in Physics Research A.
  - [8] K.-J. Kim, private communication.
  - [9] The MAD program, <http://mad.home.cern.ch/mad/>
  - [10] D. Whittum, private communication.
  - [11] C. B. Schroeder, E. Esarey and W.P. Leemans, "Electron Beam Conditioning by Thompson Scattering", Submitted for publication, October 2003.